First-principles LDA+U and GGA+U study of plutonium oxides

Bo Sun, Ping Zhang,* and Xian-Geng Zhao

Institute of Applied Physics and Computational Mathematics, P.O. Box 8009, Beijing 100088, P.R. China

The electronic structure and properties of PuO_2 and Pu_2O_3 have been studied from first principles by the all-electron projector-augmented-wave (PAW) method. The local density approximation (LDA)+U and the generalized gradient approximation (GGA)+U formalism have been used to account for the strong on-site Coulomb repulsion among the localized Pu $5f$ electrons. We discuss how the properties of PuO_2 and Pu_2O_3 are affected by the choice of U as well as the choice of exchange-correlation potential. Also, oxidation reaction of Pu_2O_3, leading to formation of PuO_2, and its dependence on U and exchange-correlation potential have been studied. Our results show that by choosing an appropriate U it is promising to correctly and consistently describe structural, electronic, and thermodynamic properties of PuO_2 and Pu_2O_3, which enables it possible the modeling of redox process involving Pu-based materials.

I. INTRODUCTION

Plutonium dioxide (PuO_2) and sesquioxide (Pu_2O_3) are the only observed stoichiometric compounds formed at the surface of the metallic plutonium when exposed to dry air[1] (nonstoichiometric oxide may form by reaction of dioxide with water[2]). From this sense, plutonium corrosion and oxidation are often treated as equivalent topic. The plutonium corrosion plays a key role in considering the nuclear stockpile and storage of surplus plutonium. Therefore, a thorough understanding of the physical and chemical properties of the plutonium oxide is always needed.

From basic point of view, it can be visualized that many physical and chemical properties of the plutonium oxide are closely related to the quantum process of localization and delocalization for Pu $5f$ electrons. Modeling of the electron localization, and thus any redox process involving plutonium, is a complex task. Conventional density functional schemes that apply the local density approximation (LDA) or the generalized gradient approximation (GGA) underestimate the strong on-site Coulomb repulsion of the Pu $5f$ electrons and consequently fail to capture the correlation-driven localization. Therefore, the $5f$ electrons in elemental Pu, as well as in Pu compounds, require special attention. One promising way to improve contemporary LDA and GGA approaches is to modify the intra-atomic Coulomb interaction through the so-called LDA+U or GGA+U approach, in which the underestimation of the intraband Coulomb interaction is corrected by the Hubbard U parameter[3,4,5]. This method has been used to discuss the equilibrium lattice parameter of bulk Pu in Ref.[6,7,8]. The choice of U is, however, not unambiguous and it is not trivial to determine its value *a priori*, though there are attempts to extract it from standard first-principles calculations. Hence, U is often fitted to reproduce a certain set of experimental data such as band gaps and structural properties.

In this paper we use the LDA+U and GGA+U schemes due to Dudarev et al.[9] to calculate the lattice parameters, electronic structure, and thermodynamic properties of PuO_2 and Pu_2O_3. We discuss how these properties are affected by the choice of U as well as the choice of exchange-correlation potential, i.e., the LDA or the GGA, and how redox processes occurred in plutonium oxide can be explored in the LDA+U and GGA+U formalism. In addition, we notice that recently there have occurred a few experimental[10,11,12] and theoretical[11,13,14,15] studies of the electronic structures of plutonium oxides. In this paper we have compared our calculated LDA/GGA+U results with those reports. Our results show that while the pure LDA/GGA (without U correction) calculations fail to describe the ground-state behaviors of the plutonium oxides, such as the insulating nature, the magnetic configuration, and the $5f$ band gap, the present LDA/GGA+U approaches with tunable Coulomb parameters can effectively remedy those failures and the consequent results fit well in the attainable experimental data[10,11,12].

This paper is organized as follows. The details of our calculations are described in Sec. II and in Sec. III we present and discuss the results. In Sec. IV, we summarize our findings.

II. METHODOLOGY OF THE CALCULATION

The calculations were performed using the projector-augmented wave (PAW) method of Blöchl[16], as implemented in the ab initio total-energy and molecular-dynamics program VASP (Vienna *ab initio* simulation program)[17,18,19,20]. PAW is an all-electron method that combines the accuracy of augmented-plane-wave methods with the efficiency of the pseudopotential approach. The PAW method is implemented in VASP with the frozen-core approximation. For the plane-wave set, a cut-off energy of 400 eV was used. The plutonium $6s$, $6p$, $7s$, and $5f$, and the oxygen $2s$ and $2p$ electrons were treated as valence electrons. The strong on-site Coulomb repulsion amongst the localized Pu $5f$ electrons are accounted for by using the formalism formulated by Dudarev *et al.*[9]. In this scheme the total LDA (GGA) energy functional

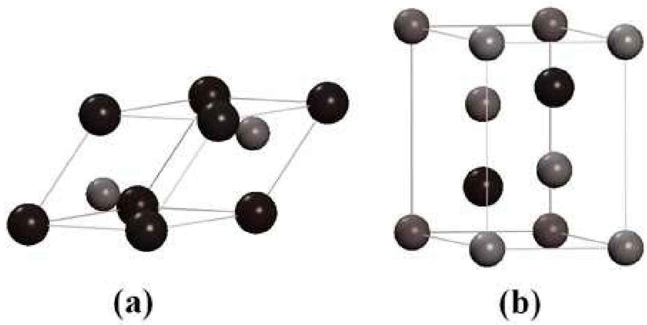

FIG. 1: (a) Unit cell of PuO_2 containing 3 atoms. The black spheres are Pu atoms, the gray ones are oxygens. (b) Unit cell of Pu_2O_3 containing five atoms.

is of the form

$$E_{\mathrm{LDA(GGA)}+U} = E_{\mathrm{LDA(GGA)}} + \frac{U-J}{2}\sum_{\sigma}\left[\mathrm{Tr}\rho^{\sigma} - \mathrm{Tr}\left(\rho^{\sigma}\rho^{\sigma}\right)\right], \tag{1}$$

where ρ^{σ} is the density matrix of f states, and U and J are the spherically averaged screened Coulomb energy and the exchange energy, respectively. In this paper the Coulomb U is treated as a variable, while the exchange energy is set to be a constant J=0.75 eV. This value of J is in the ball park of the commonly accepted one for Pu[6,21,22,23]. Since only the difference between U and J is significant[9], thus we will henceforth label them as one single parameter, for simplicity labeled as U, while keeping in mind that the non-zero J has been used during calculations.

The exchange and correlation effects were treated in both the local density approximation and the generalized gradient approximation[24]. We studied PuO_2 in its ground-state fluorite structure ($Fm3m$) and the sesquioxide Pu_2O_3 in the hexagonal β–type structure ($P\bar{3}m1$). For PuO_2 we used a $11\times11\times11$ Monkhorst-Pack k-point mesh[25] (56 irreducible k points) and for Pu_2O_3 we used a $9\times9\times6$ grid (57 irreducible k points). The electronic density of states (DOS) was obtained with $15\times15\times15$ (120 irreducible k points) and $11\times11\times9$ grid (120 irreducible k points) k-point meshes, respectively. The Brillouin-zone integration was performed using the modified tetrahedron method of Blöchl[26]. In order to study the reaction energy it is necessary to calculate the energy of an oxygen molecule (E_{O_2}). The effect of spin polarization was included in calculating E_{O_2}.

III. RESULTS AND DISCUSSION

A. Atomic and electronic structure of PuO_2

Plutonium dioxide crystallizes in a CaF_2-like ionic structure [Fig. 1(a)] with the plutonium and oxygen atoms forming face-centered and simple cubic sublattices, respectively. In this arrangement each plutonium atom is located at the center of an oxygen cube, and for every four such cubes there is an empty one. In the ionic limit, formal charge for plutonium in PuO_2 is +4, corresponding to formal population of f^4. This leads to local S=2 plutonium moment, which can couple with other sites in either a ferromagnetic (FM) or antiferromagnetic (AFM) manner. PuO_2 is known to be an insulator[27] and some scattered experimental data[28] support the ground state of PuO_2 to be an AFM phase. In the present LDA/GGA+U approaches, we have considered the FM, AFM, and nonmagnetic phases for each choice of the value of U and then determined the ground-state phase by a subsequent total-energy comparison of these three phases. For PuO_2, at U=0, the ground state is a FM metal, which is in contrast to experiment. By increasing the amplitude of U, our LDA/GGA+U calculations correctly predicted an AFM insulating ground state. The turning value of U for this FM-AFM energy transition of the ground state is of ∼1.5 eV. In the discussion that follows, we therefore confined our report to the AFM solution for the PuO_2. A thorough description of the magnetic structure of plutonium oxides is beyond our intention in this paper, and we would like to leave it for the future studies.

The experimentally determined lattice parameter of PuO_2 is a_0=5.396 Åat 25°C[29]. Here the calculated a_0 and bulk modulus B_0 of PuO_2 were obtained from the corresponding energy minimization at constant volumes and by fitting a Murnaghan equation of state[30] to the resulting energy-volume data, respectively. The results as a function of U within the LDA and the GGA schemes are shown in Fig. 2(a) and (b) for a_0 and B_0, respectively. For comparison, the experimental values of a_0[29] and B_0[31] are also shown in Fig. 2. For the pure DFT calculation (U=0), it shows in Fig. 2(a) that the LDA overbinds the compound and underestimates with respect to the experiment the lattice parameter by ∼2%, while the GGA calculation give a slight overestimate of a_0. After turning on the Hubbard U, one can see from Fig. 2(a) that for the LDA+U approach, although the lattice parameter is still underestimated in a wide range of U, the calculated a_0 for PuO_2 improves upon the pure LDA by steadily increasing its amplitude with U. In fact, at a typical value of U=4 eV, the LDA+U gives a_0=5.36 Å, which is very close to the experiment. On the other hand, with increasing U, the underbind effect brought about by the GGA+U is somewhat enlarged. As a comparison, at U=4 eV, the GGA+U gives a_0=5.47 Å, which overestimates the experimental data by ∼1.3%. Overall, both the LDA+U and GGA+U results of the lattice parameter for the PuO_2 AFM phase are comparable with experiment by tuning in the calculations the Hubbard U around 4 eV. We have also calculated the equilibrium lattice parameter for the FM and nonmagnetic phases for PuO_2. The tendency of a_0 with U for these two phases is similar to that for the present AFM phase. For the calculated bulk modulus B_0 of the PuO_2 AFM phase, one

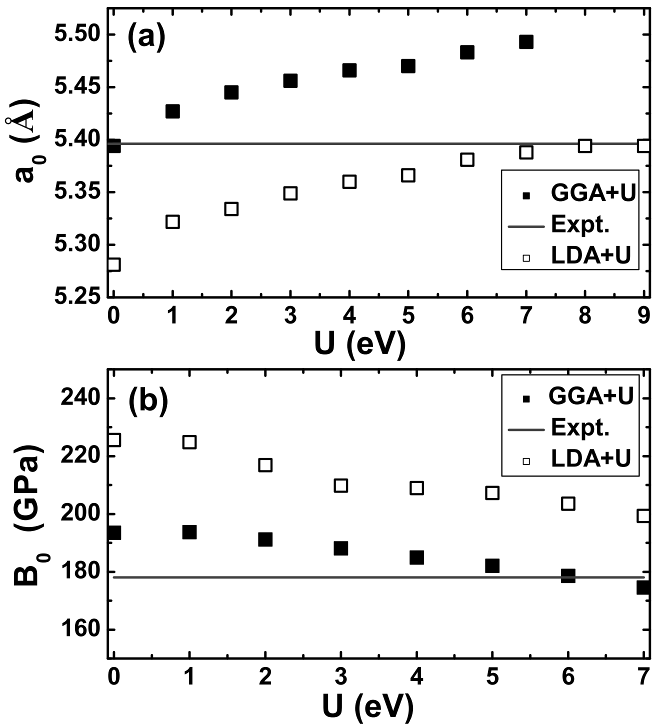

FIG. 2: Dependence of the lattice parameter (a) and bulk modulus (b) of PuO_2 on U.

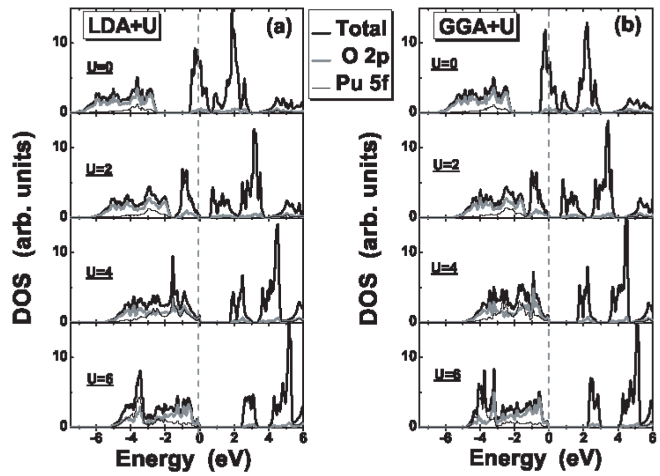

FIG. 3: The total DOS for the PuO_2 antiferromagnetic phase computed in the (a) LDA+U and (b) GGA+U formalism with four selective values of U. The projected DOS for the Pu $5f$ and O $2p$ orbitals are also shown. The Fermi level was set to be zero.

can see from Fig. 2(b) that its value varies with U over a rather broad range of 175 to 195 GPa for the GGA+U and 200 to 230 GPa for the LDA+U. The LDA result of B_0 is always higher than the GGA result, which is due to the above-mentioned "overbind" characteristics of the LDA approach. For the measurements of the equilibrium bulk modulus, there are no consistent results to date for the AFM PuO_2. Here we compared our calculation to the experimental result of B_0=178 GPa reported in Ref.[31]. One can see from Fig. 2(b) that the discrepancy between the present calculation and the experiment is most distinct at U=0. Both the LDA and the GGA give an overestimate, with the latter more close to the experimental data. By turning on the effective Coulomb interaction, the amplitude of B_0 begins to decrease. At a typical value of U=4 eV, the LDA+U gives B_0=208 GPa while the GGA+U gives B_0=184 GPa. We notice that the recent hybrid density-funtional calculations[14] predict the bulk modulus to be 220 GPa for the antiferromagnetic PuO_2, comparable with the present pure LDA results. For lattice parameter a_0 it was predicted to be 5.46 in Ref.[14]. To conclude (Fig. 2), comparing with the experimental data and the recent hybrid density-functional results, the accuracy of our atomic-structure prediction for the antiferromagnetic PuO_2 is quite satisfactory by tuning the effective Hubbard parameter U in a range 3–4 eV within the LDA/GGA+U approaches.

Besides the prominent changes in the atomic-structure parameters, the most dramatic improvement brought by the LDA/GGA+U when compared to the pure ones is in the description of electronic-structure properties. For this we have investigated the band structures of the PuO_2 AFM phase with the aim at seeing the fundamental influence by the inclusion of the on-site Coulomb interaction. The resultant total density of states (DOS) for four selective values of U are plotted in left (LDA+U) and right (GGA+U) panels in Fig. 3. For more clear illustration, the projected DOS for the Pu $5f$ and O $2p$ orbitals are also shown in Fig. 3. The Fermi energy E_F has been set to be zero. Without accounting for the on-site Coulomb repulsion (U=0), one can see that both two pure DFT methods predict an incorrect metallic ground state by non-zero occupation of Pu $5f$ states at E_F. When switching on U, as shown in Fig. 3, the Pu $5f$ band begins to split at E_F and tends to open a gap Δ. The amplitude of this insulating gap increases with increasing U, see Fig. 4. Overall the LDA+U and GGA+U give an equivalent description of the one-electron behaviors in a wide range of U. At a typical value of U=4 eV, one can see from Fig. 3 that the occupied DOS is featured by two well-resolved peaks. The narrow one near -2.0 eV is principally Pu $5f$ in character, while the broad one near -4.0 eV is mostly O $2p$. These two pronounced peaks have been observed in the recent photoemission measurements[10,12]. In addition, by increasing the amplitude of U, one prominent feature occurred in Fig. 3 is the increasing hybridization between Pu $5f$ and O $2p$ occupied states. This interesting mixing effect disappears in the cases of Pu_2O_3 (see Fig. 6 below) and UO_2[32], for which the Pu (U) $5f$ and O $2p$ occupied bands are well separated. The presence of Pu($5f$)-Pu($2p$) hybridization in PuO_2 implies a more covalent and stronger metal-ligand mixing than in Pu_2O_3 and UO_2. This phenomenon appears surprising,

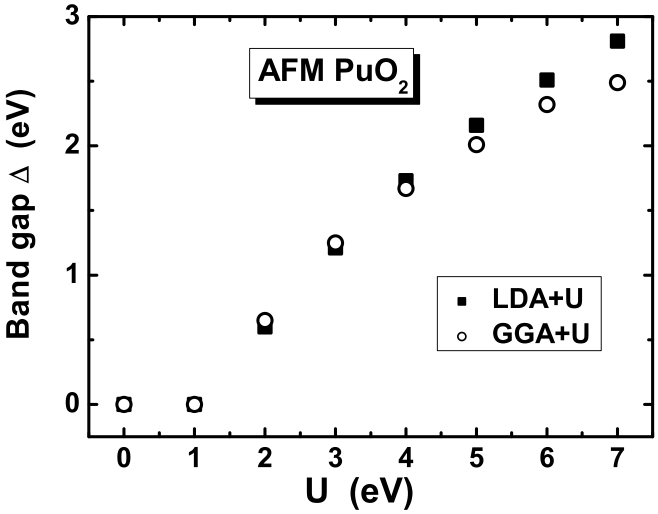

FIG. 4: The insulating band gap of the PuO_2 antiferromagnetic phase as a function of U for the LDA (filled squares) and the GGA (hollow circles).

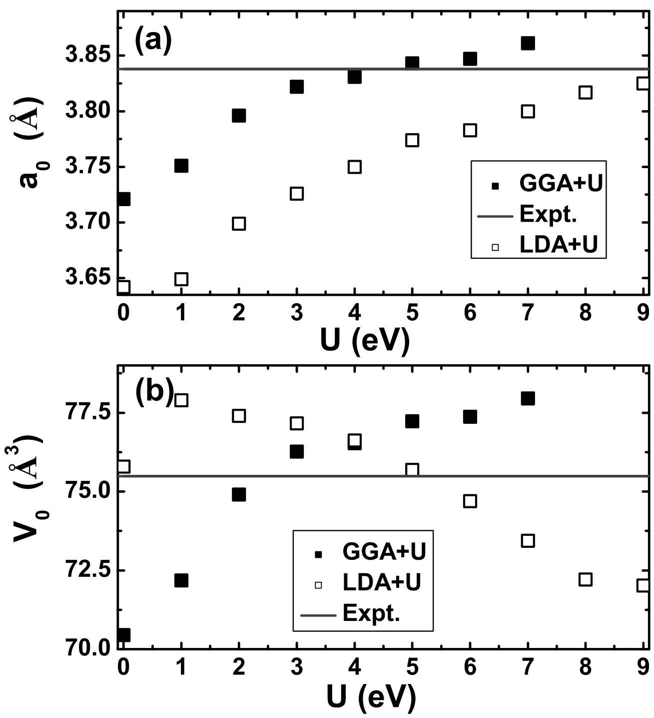

FIG. 5: Dependence of the equilibrium lattice parameter a_0 (a) and the volume V_0 of unit cell (b) of Pu_2O_3 on U.

given the smaller overlap anticipated in Pu because of the smaller radius of the Pu $5f$ orbital. Experimentally, Butterfield *et al.*[10] and Gouder *et al.*[12] have reported the thin-film photoemission data for PuO_2. The present overall picture which emerges from the LDA/GGA+U with properly selective Coulomb repulsion appear to be in satisfactory agreement with experiment. We have also compared our results given in Fig. 3 with the most recent calculations by Prodan *et al.*[14] based on newly developed screened Coulomb hybrid density functional. The agreement between our LDA/GGA+U (with U ∼4 eV) results and those in Ref.[14] is also apparent. Interestingly, the above-mentioned orbital (Pu $5f$ and O $2p$) mixing effect in PuO_2 has also been theoretically predicted by Prodan *et al.*[14,15], who hypotheses that the expected stabilization of the Pu $5f$ orbital energy relative to U $5f$ leads to an "accidental" degeneracy between the Pu $5f$ and O $2p$ levels, which in the first-order perturbation theory results in a higher degree of covalency regardless of small radius of the Pu $5f$ orbital. Therefore, although the pure LDA and GGA fail to depict the electronic structure, especially the insulating nature and the occupied-state character of PuO_2, our present results show that by tuning the effective Hubbard parameter in a reasonable range, the LDA/GGA+U approaches will prominently improve upon the pure LDA/GGA calculations and thus can provide a satisfactory qualitative electronic structure description comparable with experiments and the hybrid DFT calculation. By further increasing U to 6 eV, one can see that the peak near −2.0 eV becomes weak and is mostly O $2p$, while the peak near −4.0 eV becomes stronger and consists equally of Pu $5f$ and O $2p$ orbital. This picture of DOS is no longer valid since the peak near −2.0 eV has been confirmed to be due to the Pu $5f$ contribution. Thus the LDA/GGA+U approaches with U as large as 6 eV fails to describe the electronic structure of PuO_2.

B. Atomic and electronic structure of Pu_2O_3

Pu_2O_3 is an insulating oxide of the hexagonal β-type ($P\bar{3}m1$) [Fig. 1(b)] with space group no. 164, the only phase of the sesquioxide that has been prepared with stoichiometric composition. Both magnetic susceptibility[33] and neutron diffraction[34] measurements have found Pu_2O_3 to have an AFM structure at temperatures below 4.2 K, with the Pu moments μ confined along the $\mathbf{z}$ axis in a simple $+-+-$ alternation of spins. As with PuO_2, we have considered the FM, AFM, and nonmagnetic phases and then determined the ground-state phase by comparing the equilibrium total energies of these three phases. At U=0, the calculated ground state is as for PuO_2 an incorrect FM metal. By increasing the amplitude of U, our LDA/GGA+U approaches correctly predicted the β–Pu_2O_3 to be in an AFM insulating phase. The FM-AFM energy crossing occurs at a small U of ∼1.5 eV. We report in what follows on the Pu_2O_3 AFM phase.

The calculated equilibrium lattice parameter a_0 of Pu_2O_3 is plotted in Fig. 5(a) as a function of U. It reveals that the relation between a_0 and U does not follow a simple monotonic function. The turning point is at U=3 eV, below which a_0 goes up rapidly with U. After

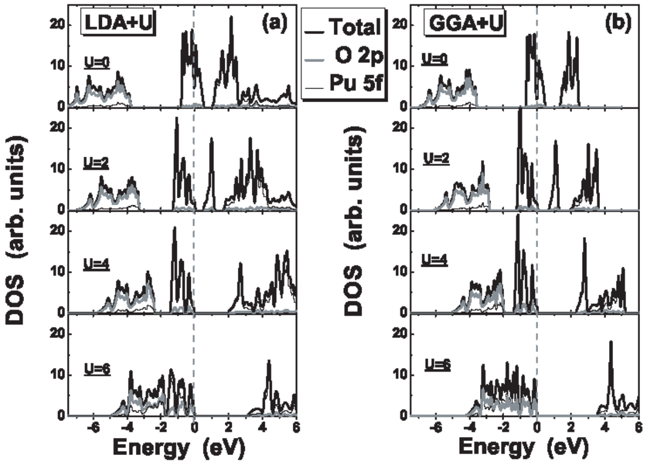

FIG. 6: The total DOS for the Pu_2O_3 antiferromagnetic phase computed in the (a) LDA+U and (b) GGA+U formalism with four selective values of U. The projected DOS for the Pu $5f$ and O $2p$ orbitals are also shown.

crossing this turning point, the increase of a_0 begins to slow down with U. Thus the curvature of a_0 for small values of U is more significant than for large values of U. The decrease in curvature at large U corresponds to the separation of the occupied Pu $5f$ band from the unoccupied part, i.e., the transition from a metallic to an insulating ground state of Pu_2O_3 (see below). This feature in the increase of a_0 as a function of U is almost the same for the LDA and the GGA. The experimental data[33,34] of a_0=3.841 Åis well fitted at U=4 eV for the GGA, while the LDA always slightly underestimates a_0. Another feature shown in Fig. 5(a) is that at small values of U below 4 eV the GGA underestimates a_0, which is contrary to the general experience that in most cases (as shown for PuO_2), the GGA often gives a slight overestimate of lattice parameter. This rarely-occurred feature may be due to the appearance of the other lattice parameter in β–Pu_2O_3, i.e., the rario c_0/a_0 for the hexagonal crystalline structure. The equilibrium volume V_0 of of the Pu_2O_3 unit cell (including 5 atoms) as a function of U is plotted in Fig. 5(b). The experimental result[33,34] of V_0 is also given for comparison. Although the tendency of V_0 with U is remarkably opposite for the two DFT+U methods, the results mostly overlap at a typical value of U=4 eV, at which insulating gap for the Pu_2O_3 is well formed. The different tendency of V_0 with respect to U for the LDA and GGA may come from sensitivity of the anisotropy in Pu $5f$ orbitals to the treatment of the exchange-correlation potential. Combining Fig. 5(a) and (b) it is expected that both the LDA and the GGA may give a satisfactory prediction of the ground-state atomic structure for the Pu_2O_3 by tuning U to be near 4 eV.

The LDA/GGA+U total DOS for the Pu_2O_3 AFM phase are shown in Fig. 6 for four selective values of U. The projected DOS for the Pu $5f$ and O $2p$ orbitals are also plotted. Both the LDA and GGA predict an incorrect metallic ground state for Pu_2O_3 at U=0 by the presence of non-zero occupation of Pu $5f$ state at the Fermi energy E_F. When turning on the on-site Coulomb repulsion, the Pu $5f$ band begins to split and form an insulating gap Δ at a critical value U=1 eV. The gap Δ becomes large with increasing U, as shown in Fig. 7, from which one can see that the amplitude of Δ for Pu_2O_3 is almost equivalent to that for PuO_2 at low U. At a typical value of U=4 eV, it reveals in Fig. 6 that the occupied DOS is featured by two peaks. The narrow one near -1.5 eV is principally Pu $5f$ in character, while the broad one around -4.0 eV is mostly O $2p$. It is encouraging that these two pronounced peaks, as well as the overall appearance of the total DOS spectrum, fit well in recent photoemission experiments[10,12] on Pu_2O_3. We have also compared our results given in Fig. 6 with the recent calculations by Prodan *et al.*[14] using the hybrid density functional. Our LDA/GGA+U results (with U $\sim$4 eV) for the Pu_2O_3 AFM phase are in excellent agreement with those in Ref.[14]. Unlike in PuO_2, the Pu $5f$ and O $2p$ states in Pu_2O_3 are well separated in the DOS spectrum. This feature is similar to that of UO_2[32], which also exhibits two distinct peaks of U $5f$ and O $2p$ parentage. Remarkably, the similar trend has also been theoretically reported on Pu_2O_3 in Ref.[14] within the hybrid-density-functional framework. A consistent explanation with the Pu($5f$)-O($2p$) hybridization in PuO_2 may sustain by understanding the orbital separation in Pu_2O_3 as a consequence of the more weakly bound Pu $5f$ site energy associated with the less highly charged Pu^{3+} ion[13]. With further increasing the effective intratomic Coulomb interaction to U=6 eV, as shown in Fig. 6, the separation of the Pu $5f$ from O $2p$ projected DOS is blurred by the increasing spectrum weight of the former around -4 eV, which overlaps largely with the O $2p$. This no longer accord with the experiments[10,12]. Therefore, as with PuO_2, the LDA/GGA+U approaches with U as large as 6 eV fail to describe the electronic structure of Pu_2O_3.

C. Oxidation reaction energy

Oxidation of Pu_2O_3 via the reaction

$$Pu_2O_3 + \frac{1}{2}O_2 \rightarrow 2PuO_2 \tag{2}$$

leads to formation of stoichiometric PuO_2. The dependence of the transformation reaction energy on U is presented in Fig. 8. One can see that both the LDA and the GGA show the same dependence of reaction energy on the on-site Coulomb interaction. That is, at small values of U which correspond to the metallic ground state for both PuO_2 and Pu_2O_3, the reaction energy is independent of U. Above the metallic-insulating transition, our calculated reaction energy decreases linearly with increasing U. The reason for this behavior is that a high

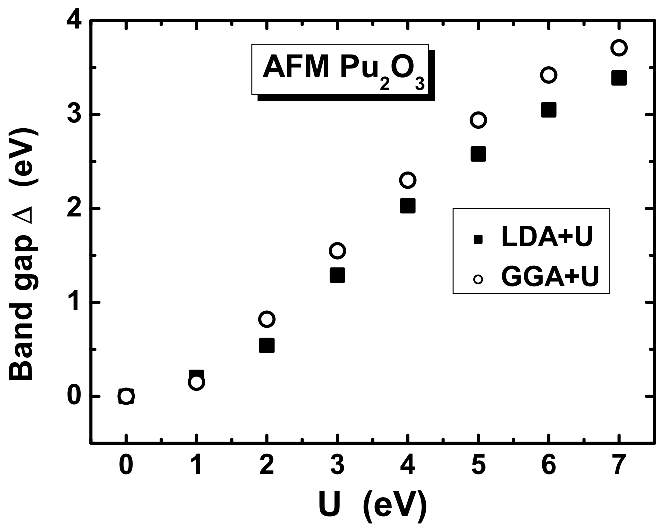

FIG. 7: The insulating band gap of the Pu_2O_3 antiferromagnetic phase as a function of U for the LDA (filled squares) and the GGA (hollow circles).

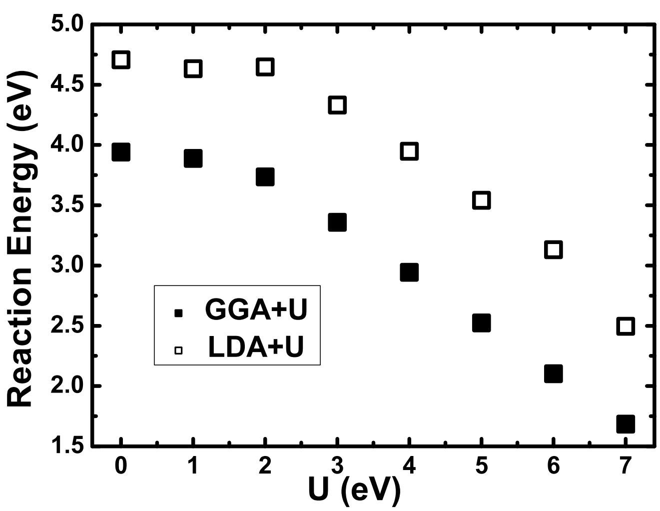

FIG. 8: Dependence of the $Pu_2O_3 + \frac{1}{2}O_2 \rightarrow 2PuO_2$ reaction energy on U.

U favors localization and thus facilitates the transition. Density functional theory is known to overestimate the binding energy of O_2 and this should result in an underestimation of the present reaction energy via the E_{O_2} term. Consequently we cannot expect a perfect agreement with experiments for the present reaction energy. However, this error is independent of any conditions in the plutonium oxide and thus can be remedied by shifting the energy of O_2 so as to give the experimental binding energy. In the LDA the O_2 binding energy is overestimated by 1.2 eV/0.5 O_2 and in the GGA the corresponding number is 0.8 eV/0.5 O_2. The GGA always predicts a lower value of the reaction energy, as seen from Fig. 9.

IV. CONCLUSIONS

We have studied the structural, electronic, and thermodynamic properties of the antiferromagnetic PuO_2 and Pu_2O_3 within the LDA+U and GGA+U frameworks. The atomic structure, including lattice parameters and bulk modulus, and the one-electron behaviors of these kinds of plutonium oxides have been systematically investigated as a function of the effective on-site Coulomb repulsion parameter U. We find that both the LDA+U and GGA+U considerably improves upon the traditional density functionals, providing a first-principles description of plutonium oxides in satisfactory qualitative agreement with experiment. Also our present results are well comparable to those obtained through newly developed hybrid DFT method. Specially, from the LDA/GGA+U study of the lattice parameter of PuO_2 we find that the experimental data of a_0 can be gradually approached by steadly increasing U to be in an acceptable range around 4 eV. The incorrect metallic ground state at purely LDA or GGA (U=0) for both PuO_2 and Pu_2O_3 can be readily corrected by a systematic inclusion of nonzero U, which forces the Pu 5f band to split at the Fermi level and thus drives the metallic-insulating transition. The insulating band gaps for PuO_2 and Pu_2O_3 have been shown as a function of U. The oxidation reaction Pu_2O_3+0.5O_2 →2PuO_2 has also been studied by systematically calculating the reaction energy as a function of U. Our results show that the oxidation process of the Pu_2O_3 is an exothermic reaction, which is mostly responsible for the experimentally observed[36] plutonium pyrophoricity at 150°C−200°C. Also we have shown that above the metallic-insulating transition, the reaction energy decreases with increasing U for the LDA and the GGA schemes. We expect these calculated results are useful for the future studies on the surface oxidation and corrosion of metallic plutonium.

Acknowledgments

This work was partially supported by NSFC under grants Nos. 10604010 and 60776063.

* Corresponding author. Electronic address: zhang_ping@iapcm.ac.cn

1 J.M. Haschke, Los Alamos Science **26**, 253 (2000).
2 J.M. Haschke, T.H. Allen, and L.A. Morales, Science **287**, 285 (2000).
3 V.I. Anisimov, J. Zaanen, and O.K. Anderson, Phys. Rev. B **44**, 943 (1991).
4 V.I. Anisimov, I.V. Solovyev, M.A. Korotin, M.T. Czyżyk,

and G.A. Sawatzky, Phys. Rev. B **48**, 16929 (1993).

[5] I.V. Solovyev, P.H. Dederichs, and V.I. Anisimov, Phys. Rev. B **50**, 16861 (1994).

[6] S.Y. Savrasov and G. Kotliar, Phys. Rev. Lett. **84**, 3670 (2000).

[7] A.B. Shick, V. Drchal, and L. Havela, Europhys. Lett. **69**, 588 (2005).

[8] A. Shick, L. Havela, J. Kolorenč, V. Drchal, T. Gouder, and P.M. Oppeneer, Phys. Rev. B **73**, 104415 (2006).

[9] S.L. Dudarev, G.A. Botton, S.Y. Savrasov, C.J. Humphreys, and A.P. Sutton, Phys. Rev. B **57**, 1505 (1998).

[10] M. Butterfield, T. Durakiewicz, E. Guziewicz, J. Joyce, A. Arko, K. Graham, D. Moore, and L. Morales, Surf. Sci. **571**, 74 (2004).

[11] M.T. Butterfield, T. Durakiewicz, I.D. Prodan, G.E. Scuseria, E. Guziewicz, J.A. Sordo, K.N. Kudin, R.L. Martin, J.J. Joyce, A.J. Arko, K.S. Graham, D.P. Moore, and L.A. Morales, Surf. Sci. 600, 1637 (2006).

[12] T. Gouder, A. Seibert, L. Havela, and J. Rebizant, Surf. Sci. 601, L77 (2007).

[13] I.D. Prodan, G.E. Scuseria, J.A. Sordo, K.N. Kudin, and R.L. Martin, J. Chem. Phys. **123**, 014703 (2005).

[14] I.D. Prodan, G.E. Scuseria, and R.L. Martin, Phys. Rev. B **73**, 045104 (2006).

[15] I.D. Prodan, G.E. Scuseria, and R.L. Martin, Phys. Rev. B **76**, 033101 (2007).

[16] P.E. Blöchl, Phys. Rev. B **50**, 17953 (1994).

[17] G. Kresse and J. Hafner, Phys. Rev. B **48**, 13115 (1993).

[18] G. Kresse and J. Furthmüller, Comput. Mater. Sci. **6**, 15 (1996).

[19] G. Kresse and J. Furthmüller, Phys. Rev. B **54**, 11169 (1996).

[20] G. Kresse and D. Joubert, Phys. Rev. B **59**, 1758 (1999).

[21] D. van der Marel and G.A. Sawatzky, Phys. Rev. B **37**, 10674 (1988); J.F. Herbst, R.E. Watson, and I. Lindgren, *ibid.* **14**, 3265 (1976).

[22] A.B. Shick, A. I. Liechtenstein, and W.E. Pickett, Phys. Rev. B **60**, 10763 (1999).

[23] A.B. Shick, V. Janiš, and P.M. Oppeneer, Phys. Rev. Lett. **94**, 016401 (2005).

[24] J.P. Perdew, J.A. Chevary, S.H. Vosko, K.A. Jackson, M.R. Pederson, D.J. Singh, and C. Fiolhais, Phys. Rev. B **46**, 6671 (1992).

[25] H.J. Monkhorst and J.D. Pack, Phys. Rev. B **13**, 5188 (1976).

[26] P.E. Blöchl, O. Jepsen, and O.K. Andersen, Phys. Rev. B **49**, 16223 (1994).

[27] C. E. McNeilly, J. Nucl. Mater. **11**, 53 (1964).

[28] P. Santini, R. Lémanski, and P. Erdõs, Adv. Phys. **48**, 537 (1999); M. Colarieti-Tosti, O. Eriksson, L. Nordström, J. Wills, and M.S.S. Brooks, Phys. Rev. B **65**, 195102 (2002); S. Kern, R. A. Robinson, H. Nakotte, G. H. Lander, B. Cort, P. Watson, and F. A. Vigil, *ibid.* **59**, 104 (1999); G. Raphael and R. Lallement, Solid State Commun. **6**, 383 (1968).

[29] R. G. Haire, J. M. Haschke, MRSBull. 689 (September 2001).

[30] F.D. Murnaghan, Proc. Natl. Acad. Sci. U.S.A. **30**, 244 (1944).

[31] M. Idiri, T. LeBihan, S. Heathman, and J. Rebizant, Phys. Rev. B **70**, 014113 (2004).

[32] K.N. Kudin, G.E. Scuseria, and R.L. Martin, Phys. Rev. Lett. **89**, 266402 (2002).

[33] B. McCart, G.H. Lander, and A.T. Aldred, J. Chem. Phys. **74**, 5263 (1981).

[34] M. Wulff and G.H. Lander, J. Chem. Phys. **89**, 3295 (1988).

[35] F.H. Ellinger, The Metal Plutonium (The University of Chicago Press, Chicago, IL, 1961).

[36] J.C. Martz, J.M. Haschke, and J.L. Stakebake, J. Nuclear Materials **210**, 130 (1994).